

# MODIFICATION OF SURFACE MORPHOLOGY AND REFRACTIVE INDEX OF A POLYMER FILM USING NEAR-FIELD SCANNING OPTICAL MICROSCOPY

Satoshi Takahashi, Hirokazu Muta, Shinjiro Machida, and Kazuyuki Horie

Department of Chemistry and Biotechnology, The University of Tokyo

7-3-1 Hongo, Bunkyo, Tokyo 113 8656, JAPAN

FAX +81 3 5841 8658, email: takasa@chembio.t.u-tokyo.ac.jp

Modification of surface morphology and refractive index as well as refractive index patterning of a polymer film has been demonstrated with near-field scanning optical microscopy (NSOM). A spin-coated film of poly(methylmethacrylate) doped with 3-phenyl-2,5-norbornadiene-2-carboxylic acid (PNCA) was used as a sample. By introducing a UV laser (325 nm) into the NSOM probe, the photoisomerization of PNCA was locally induced. After the irradiation, the topographic image and the corresponding NSOM image of the sample were collected simultaneously using a visible laser (442nm). The irradiated region, where the refractive index should decrease by the photoisomerization of PNCA, revealed the decrease in transmittance. We found that this sample also showed a change in surface morphology when the sample was irradiated with UV light and most of the PNCA molecules were photoisomerized.

Key words: near-field scanning optical microscopy (NSOM), 3-phenyl-2,5-norbornadiene-2-carboxylic acid (PNCA), refractive index, surface modification

## 1. INTRODUCTION

Nanostructure formation on the surfaces of various kinds of materials is a basic technology of so called "nanotechnology" which has recently been extensively studied. In the micrometer scale, optical techniques, including various methods of the spectroscopy and the photolithography are well-established, and they have been applied to, for example, the semiconductor industry and the biotechnology. However, if we are to apply optical techniques to the nanotechnology, there is a fundamental limitation in the spatial resolution due to the diffraction limit. Near-field scanning optical microscopy (NSOM) is one of the super-resolution techniques which can circumvent the diffraction limit[1]. One of the most powerful features of NSOM is optical spectroscopy beyond the diffraction limit, and another fascinating feature is the possibility of various applications to the nanoscale optical lithography. There are a number of modes of surface modification using NSOM, including magneto-optical effects[2], thermal effects[3], photochromism[4], etc. Among them the fabrication and the characterization of optical components on the nanometer scale should be an attractive research field which can provide basic experimental data for investigating the mechanisms of the interactions between light and nanoscale structures, in other words "optics at nanometer scale". We have investigated materials which possess large changes in refractive index induced by

photochemical reactions [5,6]. On such materials, it will be possible to create well-defined patterns of refractive index contrast, i. e. , nanolens and nanoprism by using NSOM. By selecting a wavelength that causes no photochemical reaction in the sample, NSOM images of such refractive index patterns can be obtained immediately after the surface modification. In addition, if such refractive index pattern are formed in the flat substrate, it will be possible to discuss the relation between the NSOM image and the refractive index pattern without considering the effects of surface topography. In our previous report[7], refractive index patterning without significant morphological changes was demonstrated. In the present study, by using NSOM, we demonstrate morphological modification in addition to the modification of refractive index and refractive index patterning.

## 2. EXPERIMENTAL

As a sample we used poly(methyl methacrylate) doped with 3-phenyl-2,5-norbornadiene-2-carboxylic acid (PNCA). PNCA can be photoisomerized with UV radiation such as He-Cd laser (wavelength 325 nm) to 3-phenyl-quadracyclane-2-carboxylic acid (PQCA). The scheme of the photochemical reaction of PNCA is shown in Fig. 1. PNCA was doped in a toluene solution of poly(methyl methacrylate) (PMMA). The concentration of PNCA against PMMA was about 30 wt%. This solution

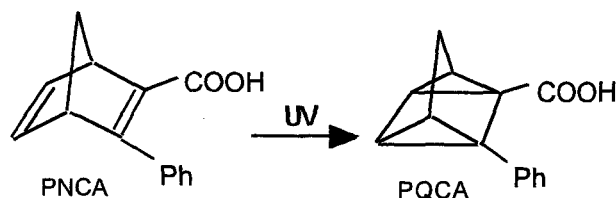


Fig. 1. Scheme of the photochemical reaction.

was spin coated onto glass substrates to make the samples. The spin-coated substrates were dried in vacuo. The thickness of the film varied from 0.3 ~ 3  $\mu\text{m}$ . A typical time dependency for an absorption spectrum of PNCA-doped PMMA film before and after the UV irradiation (325 nm) is shown in Fig. 2. The UV irradiation power density for obtaining Fig. 2 was approximately 1  $\text{mW}/\text{cm}^2$ . As shown in Fig. 2 the PNCA-doped polymer film shows no change in transparency in the visible light region, while its refractive index is, according to the results of a previous study[5], reduced by 0.006. It should also be noted that in Fig. 2, the sample was transparent at 325 nm after the 100 s irradiation.

The experimental setup is schematically illustrated in Fig. 3. The details of the setup are reported elsewhere[8]. Briefly, the beam from a He-Cd laser is coupled with the optical fiber probe of NSOM. For surface modification, the laser line with a wavelength of 325 nm is selected which is sufficiently absorbed by PNCA (See Fig. 2). A typical power density during the UV irradiation ranged from 0.03 - 4  $\text{W}/\text{cm}^2$ , depending on the tip. When collecting the NSOM image after modification, the wavelength 442 nm, for which the sample is transparent, was chosen. NSOM images were read out with the transmission mode. Although the sample does not have significant absorption at 442 nm, the refractive index variation caused by the reaction of PNCA changes the intensity of the transmitted light. The distance between the tip and the probe is regulated with the shear-force technique[9,10]. The components for the shear force detection are omitted in Fig. 3 for clarity.

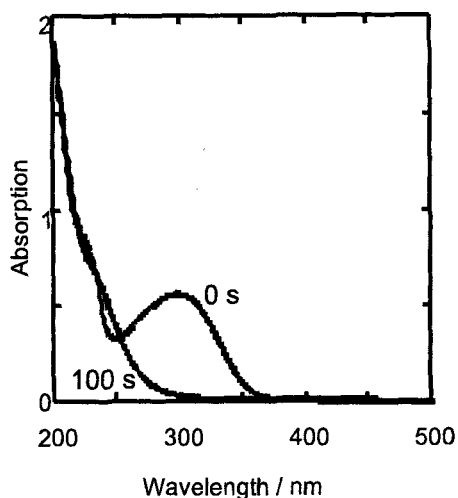


Fig. 2. Absorption spectra of the thin film of PNCA-doped PMMA before and after UV irradiation.

### 3. RESULTS AND DISCUSSION

It is possible to make a refractive index contrast using an NSOM probe without significant change of the topography. Such a demonstration is presented in Fig. 4. The fast scan axis of the images is along the vertical direction. First, the 325 nm laser light was coupled into the probe, and the probe scanned the sample along a line which is shown as line AB in Fig. 4(a). The power density of the radiation was 0.03  $\text{W}/\text{cm}^2$ . The irradiation time was 20 min. The length of the irradiated area is about 6  $\mu\text{m}$ . The width of the area (line thickness) is determined by the effective diameter of the NSOM probe and the thickness of the film. In the NSOM image a dark line is observed which corresponds to the area of relatively lower transmission. Such a line is not observed in the corresponding region in the topographic image. The contrast of the dark line is not so clear partly because of the noise in the electronics of the NSOM system and partly because of the coupling of the topographic

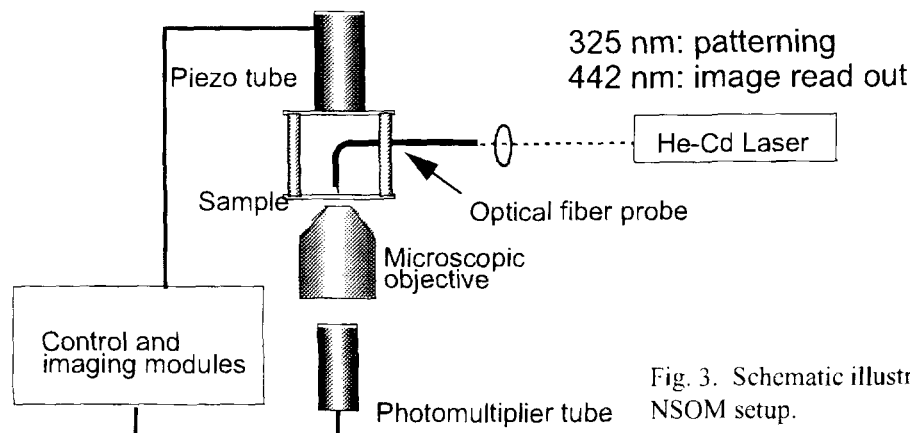


Fig. 3. Schematic illustration of the NSOM setup.

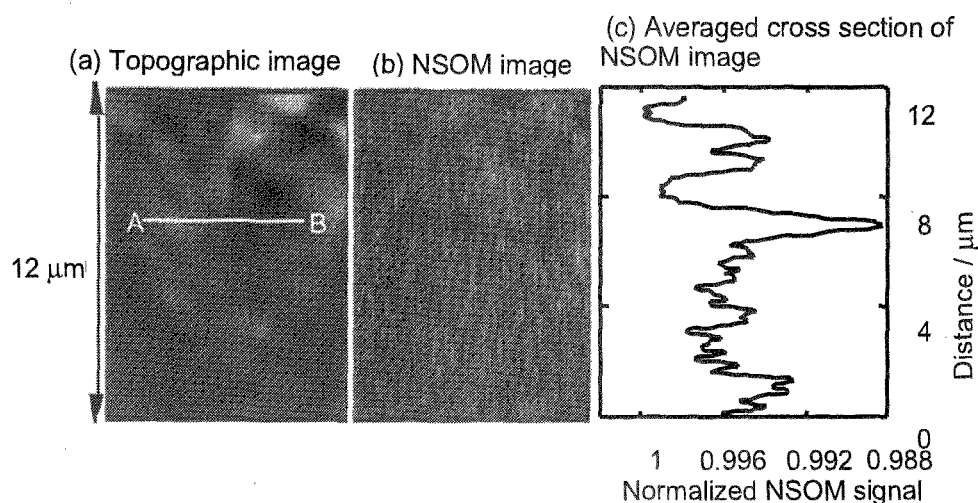


Fig. 4. Topographic image (a) and corresponding NSOM transmission image (b) of PNCA-doped PMMA thin film after UV irradiation with the NSOM probe. The probe was scanned along a horizontal line (shown by line AB in Fig. 4(a)) during the irradiation. Fig. 4(c) is an averaged profile of the NSOM image. The averaging was taken over all vertical (fast) scans that cross line AB.

effects[11, 12] from the protrusions in the scanned area. In order to elucidate the transmission contrast created in the NSOM image we displayed an averaged cross section of Fig. 4(b). The averaging was taken at each vertical distance covering the whole range parallel to line AB. The profile is shown in Fig. 4(c), where the transmittance decrease of approximately 0.8% is shown at a distance of about 7 μm, which is relevant to the irradiation area (see Fig. 4(a)). This change is significantly larger than the decrease in transmittance at the distance of 10 μm, which can be attributed to the topographic effects, and the fluctuation of the signal. As shown in Fig. 2, the sample is transparent for 442 nm light, both before and after the irradiation. The power density employed for the irradiation was sufficient for photoisomerizing most of the PNCA molecules, resulting in the decrease in refractive index in the irradiated area (along line AB). Thus, the decrease in the transmittance observed in Fig. 4 is not due to the absorption, but due to the decrease in refractive index. One explanation for the variation in transmission intensity of NSOM is to use Fresnel's relationship for the transmittance of dielectric media. According to this formula the transmission signal for the irradiated area (with a lower refractive index) should be larger than the unirradiated area. Another possible explanation is related to the scattering efficiency of the sample surface. According to this second explanation, the sample surface works as a scatterer which converts the evanescent field at the NSOM tip end into propagating light. Then the transmittance increases with the refractive index of the surface, and the irradiated area with a lower refractive index reveals a lower transmission intensity. In Fig. 4, the transmission signal of the irradiated area is relatively small. Therefore, the effect of the scattered evanescent field from the NSOM probe at the sample surface should be dominant.

Chemical reactions in the polymer materials often modify the surface morphology. The PNCA-doped PMMA films can sometimes give rise to such morphological changes, as is demonstrated in Fig. 5. The film thickness was 3 μm. The power density of the irradiation (325 nm) from the NSOM probe was approximately 4 W/cm<sup>2</sup>. The probe was moved along the line shown in the topographic image of Fig. 5 for 17 min. In the topographic image, a groove is clearly observed in the irradiated area, and in the corresponding NSOM image[Fig. 5(b)], a dark band similar to that in Fig. 4(b) is observed. In this case, contrast mechanism of the NSOM image in Fig. 5 is a coupling of two different contributions: topographic effects, and refractive index effects. For 10 min irradiation by using the same probe, the refractive index contrast was successfully formed without forming topographic contrast (the data are published elsewhere[7]).

There are three possible mechanisms to explain the morphological change in Fig. 5: mechanical damage occurring during the scan for irradiation, heat generated by the light absorption of the sample, and heat generated at the NSOM probe itself. However it is difficult to explain the morphological change in Fig. 5 simply by applying these mechanisms. First, the mechanical damaging does not occur in the present experiments. This is evidenced, as is shown in Fig. 6, by scanning the sample surface without introducing the 325 nm laser light into the NSOM probe. There is no change of the topography. Thus it can be concluded that the UV irradiation is necessary for forming a depression on the sample surface. Second, if the heat generated in the sample causes the surface morphological change, such deformation should occur most efficiently at the beginning of the irradiation, because the absorption of the sample for the UV light is largest at the beginning of the

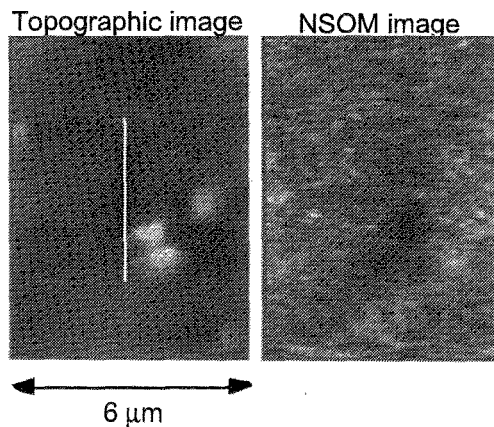


Fig. 5. Topographic image and corresponding NSOM transmission image of PNCA-doped PMMA thin film after UV irradiation with the NSOM probe. The irradiated area is along the  $4 \mu\text{m}$  vertical line located at the center of the image (shown by a white line).

irradiation. Then if we want to photoisomerize the PNCA completely, thermal damage of the sample should always occur, and it is impossible to form refractive index pattern without any topographical changes as in Fig. 4. Finally the heat generated by the probe is small enough to avoid thermal modification of the sample considering that the laser power density of  $4 \text{ W/cm}^2$  and that the laser was cw[15]. In addition, if the irradiation power is sufficiently high, the sample should be thermally damaged even in the early stage of the irradiation. Further information, including the time and power dependence of the surface modification (of both topography and refractive index) should be necessary for quantitative discussion.

#### 4. SUMMARY

Modification of surface morphology and refractive index of a polymer film has been demonstrated with NSOM. The refractive index of PNCA-doped PMMA films was changed by the evanescent field from the NSOM probe. A refractive index modification without corresponding topographic change is demonstrated. Such purely optical contrasts will provide experimental observations about the mechanisms of NSOM image formation without being obstructed by the effect of the surface topography. For some samples, changes in the surface morphology are also found. This is unfavorable if pure optical contrasts are necessary. Nevertheless, topographic features such as depressions and protrusions can act as scatterers of the surface electromagnetic waves (evanescent waves or surface plasmons on metals). By placing such topographic features in an ordered manner, they may also act as nano-optical devices. Finally, we found that the topographic changes generated by the irradiation of the UV light did not simply originate from the light absorption of the sample. Although further investigation is necessary, it is demonstrated that NSOM

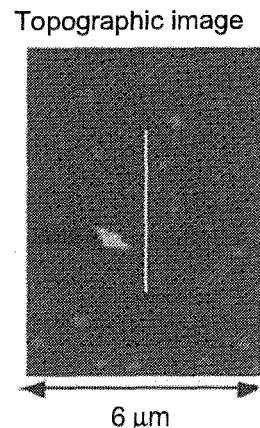


Fig. 6. Topographic image of the PNCA-doped PMMA thin film after "scratched" with the NSOM probe. The sample was scanned along the  $4 \mu\text{m}$  vertical line located at the center of the image (shown by a white line).

is applicable to the investigation of the modification of polymer thin films both from the topographical and optical viewpoints.

#### 5. REFERENCES

- [1] R. C. Dunn, *Chem. Rev.*, **99**, 2329-2927 (1999).
- [2] E. Betzig, J. K. Trautman, *Science* **257**, 189-195 (1992).
- [3] S. Hosaka, T. Shintani, M. Miyamoto, A. Hirotsune, M. Terao, M. Yoshida, K. Fujita, and S. Kammer, *Jpn. J. Appl. Phys., Part 1*, **35**, 443-447 (1996).
- [4] M. Hamano and M. Irie, *Jpn. J. Appl. Phys., Part 1*, **35**, 1764-1767 (1996).
- [5] K. Kinoshita, K. Horie, S. Morino, and T. Nishikubo, *Appl. Phys. Lett.*, **70**, 2940-2942 (1997).
- [6] S. Murase, K. Kinoshita, K. Horie, and S. Morino, *Macromolecules*, **30**, 8080-8090 (1997).
- [7] S. Takahashi, K. Samata, H. Muta, S. Machida, and K. Horie, *Appl. Phys. Lett.*, **78**, 13-15 (2001).
- [8] S. Takahashi, S. Machida, and K. Horie, *J. Photopolymer Sci. Technol.*, **13**, 231-234 (2000).
- [9] E. Betzig, P. L. Finn, J. S. Weiner, *Appl. Phys. Lett.*, **60**, 2484-2486 (1992).
- [10] R. Toledo-Crow, P. C. Yang, Y. Chen, and M. Vaez-iravani, *Appl. Phys. Lett.*, **60**, 2957-2959 (1992).
- [11] B. Hecht, H. Bielefeld, Y. Inouye, D. W. Pohl, and L. Novotny, *J. Appl. Phys.*, **81**, 2499-2503 (1997).
- [12] S. I. Bozhevolnyi, *J. Opt. Soc. Am. B*, **14**, 2254-2259 (1997).
- [13] J. K. Trautman, E. Betzig, J. S. Weiner, D. J. DiGiovanni, T. D. Harris, F. Hellman, and E. M. Gyorgy, *J. Appl. Phys.*, **71**, 4659-4663 (1992).
- [14] D. A. Higgins, D. A. Vanden Bout, J. Kerimo, and P. F. Barbara, *J. Phys. Chem.*, **100**, 13794-13803 (1997).
- [15] S. Hosaka, T. Shintani, M. Miyamoto, A. Kikukawa, A. Hirotsune, M. Terao, M. Yoshida, K. Fujita, and S. Kammer, *J. Appl. Phys.*, **79**, 8082-8086 (1996).